Probing the Depth-Dependence of Molecular Sieve Membrane Composition by Step-Scan Photoacoustic (SS-PAS) Spectroscopy

*Weontae Oh and Sankar Nair**

School of Chemical & Biomolecular Engineering, Georgia Institute of Technology

311 Ferst Drive NW, Atlanta GA 3032-0100, USA

**E-mail: sankar.nair@chbe.gatech.edu*

ABSTRACT

We report the quantitative, non-destructive determination of the concentration profile of an organic molecule in a nanoporous polycrystalline zeolite molecular sieve membrane, by step scan infra-red photoacoustic experiments and analysis. An important application of step-scan photoacoustic spectroscopy is the transport-model-independent experimental description of membrane transport, by simultaneous measurement of the concentration profile, membrane thickness and membrane flux. A heterogeneous zeolite membrane model system was constructed by growing a zeolite MFI layer on a macroporous α-alumina substrate. Step scan photoacoustic spectroscopy is then used with a large range (10-500 Hz) of incident signal modulation frequencies to obtain a series of depth-dependent infra-red spectra.

Ordered nanoporous materials deposited in the form of 1-100 micron films or membranes are receiving a great deal of attention for a range of technological applications[1-4] including molecular sieving membranes for separations, catalytic membrane reactors, and templates for guest materials such as nanowires, nanotubes and nanoclusters. The knowledge of spatially-resolved membrane composition, particularly the distribution of the guest species as a function of depth, is highly desirable in these applications. However, quantitative profiling methods such as energy-dispersive X-ray analysis and IR microscopy are destructive (i.e. they require cross-sectioning the sample). Moreover, the microscopic mass transport properties of guest species in molecular sieving membranes depend strongly on their local concentration[5]. Since intra-membrane concentration profiles have thus far been inaccessible experimentally, theoretical models (e.g., Maxwell-Stefan, atomistic, or mesoscopic) are required to interpret available experimental information (*viz.* the trans-membrane flux measured at different feed pressures and temperatures)[6,7]. One important application of step-scan photoacoustic spectroscopy is the transport-model-independent characterization of membrane transport by simultaneous measurement of the permeant concentration profile, membrane thickness, and trans-membrane flux.

In this work we experimentally demonstrate for the first time the quantitative, non-destructive measurement of concentration profile of TPA structure directing species in a nanoporous model zeolite MFI membrane system. We exploit the technique of step scan photoacoustic spectroscopy (SSPAS)[8-10] for this purpose. In SSPAS, infra-red radiation modulated (chopped) at an acoustic frequency (in the 5-1000 Hz range) is absorbed by a sample and converted to heat, which propagates out of the sample as an acoustic wave to

create modulated pressure in the gas surrounding the sample in the cell. This signal is detected by a sensitive microphone and transformed to an infra-red spectrum. The depth (μ_s) over which the thermal signal is generated, is directly related to the modulation frequency (*f*) as $\mu_s = (\alpha/\pi f)^{1/2}$. Here α is the thermal diffusivity (m^2/s) of the material. Depth-dependent information can be obtained by varying the modulation frequency. The use of a step scan interferometer allows the chosen modulation frequency to provide the same sampling depth over the entire spectral range. We first derive a simple analytical expression describing the strength of the photoacoustic signal from a membrane of continuously varying composition, and discuss its application in conjunction with SSPAS measurements to concentration-profile a model zeolite MFI[11] membrane system.

The photoacoustic signal density arising from a depth *x* in the sample, taking into account incident light absorption as well as propagation of the resultant acoustic wave through the solid, is given by[9]:

$$I = \beta e^{-\beta x} e^{-x/\mu_s} \tag{1}$$

where β is the optical absorption coefficient (or alternatively, the sum of absorption coefficients associated with each of the vibrational bands of the solid) . The optical absorption length μ_β, is defined as $\mu_\beta = 1/\beta$. For a thermally homogeneous (i.e. thermal diffusivity practically constant with depth) and optically heterogeneous (i.e. depth-dependent optical absorption) sample, the photoacoustic signal intensity (Q) for a particular sampling depth can be expressed as:

$$Q = K\int_0^{\mu_s} \beta e^{-\left(\beta+\mu_s^{-1}\right)x} dx \tag{2}$$

where *K* is a system-dependent constant. For the case of an organic-templated zeolite membrane, we now express the local absorption coefficient at depth *x*, as $\beta = \beta_0 + \beta_1 C(x)$, where β_0 is the optical absorption coefficient of the inorganic zeolite membrane, β_1 is the absorption coefficient per unit concentration of the organic guest species, and *C*(*x*) the depth-dependent concentration if the guest species. Equation (2) becomes:

$$Q = K\int_0^{\mu_s} (\beta_0 + \beta_1 C(x)) e^{-\left(\beta_0+\beta_1 C(x)+\mu_s^{-1}\right)x} dx \tag{3}$$

Equation (3) can be conveniently used to depth-profile a membrane with an unknown concentration profile. This can be done by writing the integral as a discretized summation over a number of layers, each representing increments in the sampling depth. By carrying out SSPAS experiments at progressively decreasing modulation frequencies (i.e. progressively increasing sampling depths), the concentration within each incremental layer can be determined sequentially. Here we demonstrate a case where an analytical solution of (3) is used with a deliberately engineered concentration profile. A double-layered membrane (Figure 1a) is constructed, composed of an upper membrane layer with an evenly distributed guest species and a lower layer without guest species, supported on a substrate. For this system, *C(x)* is a step function with magnitude C_0 ($0<x<L_1$) or zero ($x>L_1$). The host membrane concentration is constant upto a depth L_2 and zero beyond. Figure 1b shows a schematic of the membrane.

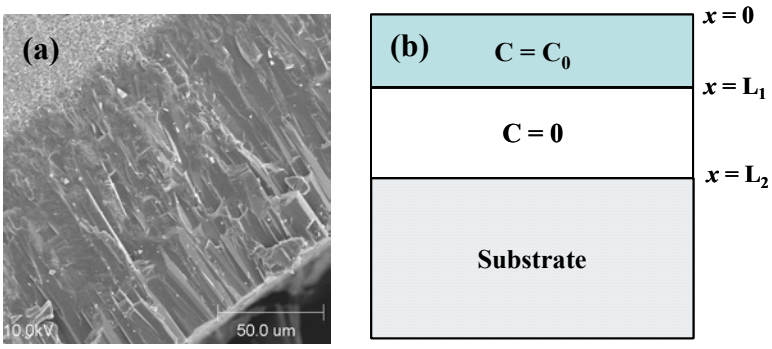

Figure 1. (a) FE-SEM image of the cross-section of a heterogenous MFI membrane, after SSPAS experiments were performed. (b) Schematic of a double-layered zeolite membrane

Since the membrane thickness (~ 100 μm) is small compared to the thickness of the substrate (~ 1.5 mm), the membrane is characterized as 'optically transparent' (i.e. IR radiation is absorbed throughout the membrane thickness). Zeolite materials have low thermal diffusivities[12,13] (α < 10^{-6} m^2/s) so that the membrane is also characterized as 'thermally thick' (i.e. the thermal diffusion length μ_s << μ_β, the optical absorption length)[9,14]. With these simplifications, Equation (3) in the region $0<\mu_s<L_1$ reduces to:

$$Q \cong K\beta_0 \int_0^{\mu_s} e^{-\mu_s^{-1}x}dx + K\beta_1 \int_0^{\mu_s} C_0 e^{-\mu_s^{-1}x}dx \; = K\mu_s\left(1-e^{-1}\right)\beta_0 + K\mu_s\left(1-e^{-1}\right)\beta_1 \qquad (4)$$

The first term is the contribution from the inorganic membrane and the second term from the guest species. Therefore, the ratio of signal intensity from the guest and the host is a constant:

$$\frac{Q_o}{Q_m} = \frac{K\mu_s(1-e^{-1})\beta_1 C_0}{K\mu_s(1-e^{-1})\beta_0} = \frac{\beta_1 C_0}{\beta_0} \qquad (5)$$

where subscripts *o* and *m* represent the organic guest and membrane respectively. Similarly when $L_1<\mu_s<L_2$,

$$\frac{Q_o}{Q_m} = \frac{K\mu_s(1-e^{-(L_1/\mu_s)})\beta_1 C_0}{K\mu_s(1-e^{-1})\beta_0} = \frac{\beta_1 C_0(1-e^{-(L_1/\mu_s)})}{\beta_0(1-e^{-1})} \qquad (6)$$

and when $\mu_s > L_2$,

$$\frac{Q_o}{Q_m} = \frac{K\mu_s(1-e^{-(L_1/\mu_s)})\beta_1 C_0}{K\mu_s(1-e^{-(L_2/\mu_s)})\beta_0} = \frac{\beta_1 C_0(1-e^{-(L_1/\mu_s)})}{\beta_0(1-e^{-(L_2/\mu_s)})} \qquad (7)$$

Equations (5), (6), and (7) describe the photoacoustic signal intensity over a range of sampling depths.

The substrate (~ 1.5 mm thickness, 10 mm dia.) for zeolite MFI membrane growth was made from α-Al_2O_3 (Alcoa A-16) powder using a hydraulic press, fired in furnace, and then polished. The silicalite (MFI) seed suspension (particle size ~ 200 nm) was synthesized as described elsewhere[15]: The seed suspension was thoroughly sonicated and filtered before

use. The zeolite MFI membrane was prepared by secondary growth. The silicate seeds were deposited on a polished porous alumina substrate and then grown hydrothermally into a membrane at 175 ^{o}C. A growth solution of composition 76.6 g DI water: 0.235 g KOH (Fisher Scientific): 1.08 g TPABr (Aldrich) : 3.77 g TEOS was used. A membrane grown for 48 hrs was then calcined at 500 ^{o}C for 6 hours to remove TPA. A heterogeneous (double-layered) zeolite membrane model system (Figure 1) was prepared by growing a second zeolite MFI layer on the completely calcined membrane layer with a fresh growth solution. The membrane was washed repeatedly with hot DI water after each synthesis step. SSPAS experiments were carried out on an IFS-55 FTIR spectrometer (Bruker) with an MTEC 300 photoacoustic detection module. Modulation frequencies were chosen in the range 11 – 418 Hz and with an amplitude of $4\lambda_{HeNe}$. After the SSPAS experiments, the membrane was cross-sectioned and imaged (Figure 1a) by field-emission SEM (Hitachi S800, 10 kV).

Figure 2a shows a series of SSPA spectra of the zeolite MFI membrane at several modulation frequencies 11 - 418 Hz. The spectral peaks are assigned on the basis of earlier literature[16] on the infra-red spectra of the MFI/TPA complex. The C-H bending and stretching vibrations (~1382, 1469, 2890, 2945 and 2980 cm^{-1}) of TPA are strongly apparent, as also the vibrations of the zeolite framework in the 1250 – 800 cm^{-1} region. As the modulation frequency increases, the sampling depth and the hence the PA signal intensity decreases correspondingly. The spectra are deconvoluted into the vibrational band components as shown in Figure 2b. The bands in the regions of 3600 - 2600 cm^{-1} and 1600 - 600 cm^{-1} are deconvoluted by non-linear least squares, assuming Gaussian and Lorentzian curve shapes respectively. The characteristic bands of the TPA-templated zeolite membrane are assigned to 1390, 1468, 2892, 2945, and 2980 cm^{-1} for TPA and 788, 981, 1053, 1185, and 1264 cm^{-1} for MFI. The integrated intensities of the 2892, 2945 and 2980 cm^{-1} (TPA) and 788 cm^{-1} (MFI) were used for quantitative analysis, as these are relatively isolated from other bands and hence free from any errors related to correlations with other band intensities.

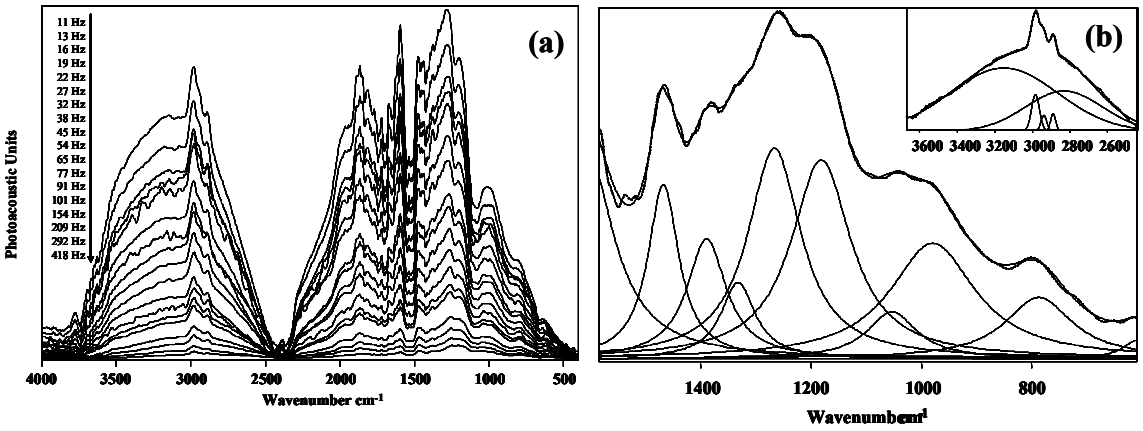

Figure 2. (a) Series of SSPA magnitude spectra collected at different modulation frequencies from the double-layered MFI membrane. (b) Representative spectrum (at 101 Hz) along with the deconvoluted components.

Figure 3a shows a log-log plot of PA intensity of the chosen MFI component versus the modulation frequency. For modulation frequencies greater than 16 Hz, The PA intensity of the MFI band decreases linearly with increasing modulation frequency on the log scale, as expected in the case of a membrane whose zeolite component is uniformly distributed along its thickness. As modulation frequency is decreased below 16 Hz, the sampling depth exceeds the membrane thickness and the intensity levels off abruptly since the entire membrane thickness is now being sampled. Using the transition frequency of 16 Hz, we estimate the

membrane thickness as 119 μm. For comparison, the membrane thickness obtained by (destructive) FE-SEM imaging of the cross-sectioned membrane is found to be 120 μm, which is in very good agreement with the PA result. Figure 3b shows the ratio of the TPA and MFI band intensities as a function of the sampling depth. It shows three regions as predicted by the theory (Equations (5), (6) and (7)) – (I) of constant TPA:MFI ratio, (II) with an exponentially decaying ratio, and (III) with a low, almost constant TPA:MFI ratio. Having estimated the overall membrane thickness (L_2), we fit Equations (5), (6), and (7) simultaneously to the data by nonlinear least squares, to obtain L_1 (the thickness of the TPA-containing layer) and $\beta_1 C_0/\beta_0$. The best fit of the model is indicated in Figure 3b, with the parameters $\beta_1 C_0/\beta_0$ = 0.5674 $\pm$ 0.063 and L_1 = 39 $\pm$ 2 μm. The fitted curve captures very well the qualitative features of the data, and also gives a reasonably good quantitative fit. It is hence found that the bottom layer has a thickness (L_2-L_1) of 80 μm. Although both layers were grown with the same reaction time, the thicknesses are not necessarily equal. The early growth starting from the randomly oriented seeds is fast. At a later stage the growth slows down since only the grains oriented with their fastest-growing direction normal to the substrate will survive[17,18]. Since the second layer is grown on top of an already existing MFI layer, the growth rate of this layer would be slower. PA intensities of Region III in Figure 3b are somewhat lower than the fitted values. This is likely due to the difference in thermal diffusion coefficient between the porous alumina substrate and the zeolite layer, and diffuse scattering of light incident at the porous substrate interface.

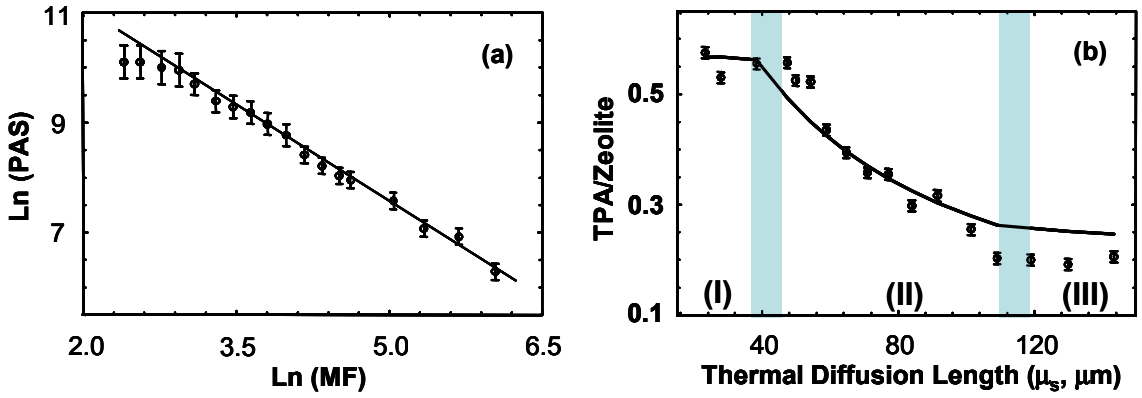

Figure 3. (a) Log-log plot of the integrated intensity of the characteristic zeolite band vs. the modulation frequency. (b) Depth profile of TPA:MFI intensity ratio in the double-layered zeolite MFI membrane sample. Region (I) TPA-templated layer, (II) calcined layer, and (III) substrate.

In conclusion, our main focus in this work was to show that SSPAS experiments and data analysis in conjunction with photoacoustic signal generation theory, constitute a viable means of non-destructively and quantitatively concentration-profiling a molecular sieve membrane. This capability is of high relevance to the understanding of structure-function relationships which govern the applications of these materials as energy-efficient separations devices and nanostructured host materials. We are currently incorporating theoretical and experimental improvements to allow more precise quantitative agreement between experimental data and fitted results. We then intend to apply the method to membranes under a permeation-induced concentration gradient.

We acknowledge the Georgia Institute of Technology for support of this research. W. Oh also thanks the Korea Science & Engineering Foundation (KOSEF) Postdoctoral Fellowship Program for partial financial support.

REFERENCES

(1) Davis, M. E. *Nature* **2002**, *417*, 813.
(2) Lai, Z. P.; Bonilla, G.; Diaz, I.; Nery, J. G.; Sujaoti, K.; Amat, M. A.; Kokkoli, E.; Terasaki, O.; Thompson, R. W.; Tsapatsis, M.; Vlachos, D. G. *Science* **2003**, *300*, 456.
(3) Mukhopadhyay, K.; Koshio, A.; Tanaka, N.; Shinohara, H. *Japanese Journal of Applied Physics Part 2-Letters* **1998**, *37*, L1257.
(4) Tsapatsis, M. *AIChE Journal* **2002**, *48*, 654.
(5) Karger, J.; Ruthven, D. M. *Diffusion in Zeolites*; John Wiley & Sons: New York, 1992.
(6) Paschek, D.; Krishna, R. *Langmuir* **2001**, *17*, 247.
(7) Kärger, J.; Vasenkov, S.; Auerbach, S. M. Diffusion in Zeolites. In *Handbook of Zeolite Science and Technology*; S. M. Auerbach, K. A. C. a. P. K. D., Ed.; Marcel Dekker: New York, 2003; pp 341.
(8) Rosencwaig, A.; Gersho, A. *Science* **1975**, *190*, 556.
(9) Rosencwaig, A.; Gersho, A. *Journal of Applied Physics* **1976**, *47*, 64.
(10) Jiang, E. Y. *Spectroscopy* **2002**, *17*, 22.
(11) Baerlocher, C.; Meier, W. M.; Olson, D. H. *Atlas of Zeolite Framework Types*, 5 ed.; Elsevier: Amsterdam, 2001.
(12) Murashov, V. V. *Journal of Physics-Condensed Matter* **1999**, *11*, 1261.
(13) Murashov, V. V.; White, M. A. *Materials Chemistry and Physics* **2002**, *75*, 178.
(14) Gonon, L.; Mallegol, J.; Commereuc, S.; Verney, V. *Vibrational Spectroscopy* **2001**, *26*, 43.
(15) Xomeritakis, G.; Nair, S.; Tsapatsis, M. *Microporous and Mesoporous Materials* **2000**, *38*, 61.
(16) Geus, E. R.; Jansen, J. C.; van Bekkum, H. *Zeolites* **1994**, *14*, 82.
(17) Gouzinis, A.; Tsapatsis, M. *Chemistry of Materials* **1998**, *10*, 2497.
(18) Bonilla, G.; Vlachos, D. G.; Tsapatsis, M. *Microporous and Mesoporous Materials* **2001**, *42*, 191.